Articles

ST7 Is a Novel Low-Density Lipoprotein Receptor-Related Protein (LRP) with a Cytoplasmic Tail that Interacts with Proteins Related to Signal Transduction Pathways†

Michele A. Battle,‡ Veronica M. Maher, and J. Justin McCormick*

Carcinogenesis Laboratory, Cell and Molecular Biology Program, Department of Biochemistry and Molecular Biology, and Department of Microbiology and Molecular Genetics, Michigan State University, East Lansing, Michigan 48824-1302

Received January 15, 2003; Revised Manuscript Received April 8, 2003

ABSTRACT: In 1997, McCormick and co-workers identified a novel putative tumor suppressor gene, designated *ST7*, encoding a unique protein with transmembrane receptor characteristics [Qing et al. (1999) *Oncogene 18*, 335−342]. Using degenerate primers corresponding to the highly conserved region of the ligand-binding domains of members of the low-density lipoprotein receptor (LDLR) superfamily, Ishii et al. [*Genomics* (1998) *51*, 132−135] discovered a low-density lipoprotein receptor-related protein (LRP) that closely resembles ST7. Later, another LRP closely resembling ST7 and LRP3 was found (murine LRP9) [Sugiyama et al. (2000) *Biochemistry 39*, 15817−15825]. These results strongly suggested that ST7 was also a novel member of the low-density lipoprotein receptor superfamily. Proteins of this superfamily have been shown to function in endocytosis and/or signal transduction. To evaluate the relationship of ST7 to the LDLR superfamily proteins and to determine whether ST7 may function in endocytosis and/or signal transduction, we used proteomic tools to analyze the functional motifs present in the protein. Our results indicate that ST7 is a member of a subfamily of the LDLR superfamily and that its cytoplasmic domain contains several motifs implicated in endocytosis and signal transduction. Use of the yeast two-hybrid system to identify proteins that associate with ST7's cytoplasmic domain revealed that this domain interacts with three proteins involved in signal transduction and/or endocytosis, viz., receptor for activated protein C kinase 1 (RACK1), muscle integrin binding protein (MIBP), and SMAD anchor for receptor activation (SARA), suggesting that ST7, like other proteins in the LDLR superfamily, functions in these two pathways. Clearly, ST7 is an LRP, and therefore, it should now be referred to as LRP12.

To define the number and nature of genetic and/or epigenetic changes required to turn a normal human cell into a malignant cell, McCormick and Maher (*1*) developed a model system in which normal human fibroblasts in culture can be transformed into malignant fibroblasts by acquiring a series of genetic changes, each conferring a growth advantage that allows sequential clonal expansion. In 1997, McCormick and co-workers (*2*), using differential mRNA display to compare an infinite life span nontumorigenic human fibroblast cell strain with its carcinogen-transformed, malignant derivative, identified a transcript whose expression was lost in the latter cells. Comparison of the transcript's sequence to known gene sequences revealed that it was novel. The protein encoded by the gene, designated *ST7*, had the characteristics of a transmembrane receptor. As compared to the level of expression in the parental cell strain, *ST7* was strongly down-regulated in the tumorigenic cell line. Several malignant cell lines derived from patients' fibrosarcomas also were found to have a low level of ST7, suggesting that *ST7* is a tumor suppressor gene. Support for this hypothesis comes from the results of recent studies from this laboratory, to be published elsewhere, showing that expression of ST7 protein in a patient's fibrosarcoma-derived cell line inhibited its tumor-forming ability. Expression of a truncated ST7 protein, lacking most of the C-terminus, failed to do so.

At the time the novel gene *ST7* was discovered, Qing et al. (*2*) recognized that the protein it encoded had the characteristics of a transmembrane protein, but no other proteins with significant similarity to ST7 had been reported. About a year later, Yamamoto and co-workers (*3*), using degenerate oligonucleotides corresponding to the highly conserved region of the ligand-binding domains of members of the low-density lipoprotein receptor (LDLR)[1] superfamily, discovered a novel gene coding for a LDLR-related protein (LRP), which they designated *LRP3.* After the sequence of

† Supported by United States Department of Health and Human Services NIH Grants AG11026 and CA82885 (J.J.M.), by a grant from the Elsa U. Pardee Foundation (J.J.M.), and by a Barnett Rosenberg Fellowship (M.A.B.).

* To whom correspondence should be addressed. Phone: (517) 353-7785. Fax: (517) 353-9004. E-mail: mccormi1@msu.edu.

‡ Present address: Department of Cell Biology, Neurobiology, and Anatomy, Medical College of Wisconsin, Milwaukee, WI 53226.

10.1021/bi034081y CCC: $25.00
Published on Web 05/30/2003

LRP3 had been submitted to the databases, our search of databases for proteins structurally related to ST7 revealed a very strong similarity between LRP3 and ST7, enabling us to recognize that, although ST7 differed significantly from the LDLR prototype, it also was an LRP. Although proteins of the LDLR superfamily are best known as endocytic receptors (reviewed in refs *4*−*6*), recent studies show that the cytoplasmic domains of LRP1, LRP2, LRP5, LRP6, LDLR, VLDLR, and ApoER2 interact with a variety of adaptor and scaffold proteins implicated in signal transduction (reviewed in refs *7*−*9*).

To evaluate ST7's relationship to the proteins of the LDLR superfamily and to determine whether ST7 functions in endocytosis and/or signal transduction, we used proteomic tools, including similarity searches, sequence alignments, pattern and profile searches, and posttranslational modification prediction programs to analyze the functional motifs present in ST7. Such analyses showed that ST7 is a novel member of a subfamily of the LDLR superfamily and that similar to LDLR and other LDLR-related proteins, ST7's cytoplasmic domain contains several motifs implicated in endocytosis and/or signal transduction. To identify intracellular proteins that interact with ST7's cytoplasmic domain, we used the yeast two-hybrid system. We found that ST7's cytoplasmic domain interacts with several proteins involved in signal transduction and/or endocytosis, suggesting that ST7 functions in these pathways.

EXPERIMENTAL PROCEDURES

Materials. The sources of specific materials used are: restriction enzymes and T4 DNA ligase, New England Biolabs or Invitrogen; shrimp alkaline phosphatase, Promega; *Pfu* polymerase, Stratagene; oligonucleotides, the Michigan State University Macromolecular Structure, Sequencing, and Synthesis Facility; yeast culture medium, Clontech; and antibiotics, Sigma or Roche Molecular Biochemicals.

Cell Culture. SHAC cells, a cell line derived from a patient's fibrosarcoma, and all SHAC-derived cell strains were cultured in Eagle's minimal essential medium supplemented with 0.2 mM L-aspartic acid, 0.2 mM L-serine, and 1.0 mM sodium pyruvate, and containing 10% (v/v) supplemented calf serum, penicillin (100 units/mL), streptomycin (100 μg/mL), and hydrocortisone (1 μg/mL) in a 37 °C humidified incubator with 5% CO_2 in air. HEK 293-T cells were similarly cultured as above but using high-glucose Dulbecco's modified Eagle's medium containing 10% (v/v) fetal calf serum (HyClone).

Isolation of ST7 cDNA. To isolate full-length *ST7* cDNA, the GeneTrapper cDNA Positive Selection System (Invitrogen) and SuperScript human heart cDNA library (Invitrogen) were used according to the manufacturer's directions. Briefly, single-stranded phagemid DNA was generated by digesting double-stranded phagemid DNA (5 μg) with bacteriophage f1 gene II protein (a site-specific F1 endonuclease) and *Escherichia coli* exonuclease III. A biotinylated ST7-specific probe (5′-TTGCTCTTGCTTTTCCTCGCTGGGG-3′) was hybridized with single-stranded DNA for 1 h at 37 °C. Following hybridization, streptavidin paramagnetic beads were used to capture *ST7* cDNA−probe complexes. After several washes, single-stranded DNA bound to the beads was eluted. To produce double-stranded DNA, captured DNA was repaired using the provided repair enzyme and the same unbiotinylated *ST7*-specific oligonucleotide used in the capture procedure. Repaired DNA was electroporated into ultracompetent ElectroMax DH10B *E. coli* (Invitrogen) and plated on LB agar plates containing 100 μg/mL ampicillin. DNA isolated from several colonies was screened for the presence of a full-length *ST7* cDNA insert by restriction endonuclease digests and by sequencing the 5′ and 3′ ends. The phagemid containing *ST7* was designated pCMV-SPORT-ST7.

DNA Sequencing. The sequence of DNA samples was determined in one of three ways: manually determined using a TAQuence cycle sequencing kit (US Biochemicals) or Fidelity DNA sequencing kit (Oncor); automatically sequenced using a Visible Genetics Gene Clipper sequencer with either a ThermoSequenase Cy 5.5 terminator cycle sequencing kit or a ThermoSequenase primer (Cy 5.0 or Cy 5.5) cycle sequencing kit (Amersham); or sequenced by the Michigan State University Genomics Technology Support Facility.

Preparation of Plasma Membrane-Enriched Fractions and Western Blotting Analysis. Cells were washed in cold PBS, collected in hypotonic lysis buffer (10 mM Tris-HCl, pH 7.4, 35 mM NaF, 5 mM $MgCl_2$, 1 mM EGTA, 1 mM Na_3VO_4, 1 mM sodium pyrophosphate, 1 mM phenylmethylsulfonyl fluoride, 25 μg/mL aprotinin), and incubated on ice for 10 min. Cells were homogenized by 30 strokes in a dounce homogenizer. Homogenates were centrifuged (500*g*) for 5 min at 4 °C. Supernatants were centrifuged (16 900*g*) for 1 h at 4 °C. Pellets, which are enriched with plasma-membrane proteins, were resuspended in RIPA buffer (50 mM Tris-HCl, pH 7.5, 150 mM NaCl, 1% Triton X-100, 0.1% sodium dodecyl sulfate, 0.5% sodium deoxycholate, 1 mM EDTA, 1 mM Na_3VO_4, 2 mM phenylmethylsulfonyl fluoride, and 25 μg/mL aprotinin). To obtain cytosolic, soluble fractions, the supernatants were clarified by centrifugation (100 000*g*) for 2 h at 4 °C. The concentration of protein in each fraction was determined using a bicinchoninic acid (BCA) protein assay reagent kit (Pierce) following the manufacturer's instructions. Aliquots of each plasma membrane-enriched fraction and cytosolic, soluble fraction containing 20 μg of protein were denatured in 5X Laemelli sample buffer, separated by SDS−PAGE, and transferred to Immobilon-P membrane (Millipore). Such membranes were blocked for 2 h with Tris-buffered saline containing 0.1% Tween-20 and 5% nonfat milk (blocking solution). Blocked membranes were incubated with a monoclonal V5 antibody (Invitrogen) or a monoclonal Na^+/K^+ antibody (Affinity BioReagents, M7-PB-E9) diluted in the blocking solution for at least 2 h at room temperature and with the appropriate horseradish peroxidase-conjugated secondary antibody (Santa Cruz Biotechnology or Sigma) diluted in

[1] Abbreviations: CUB, complement factor C1s/C1r, urchin embryonic growth factor, bone morphogenetic protein; HA, hemagglutinin; HEK 293-T, human embryonic kidney 293-T; LDLR, low-density lipoprotein receptor; LDLRA, low-density lipoprotein receptor type A; LRP, low-density lipoprotein receptor-related protein; MIBP, muscle integrin binding protein; PBS, phosphate-buffered saline; PDGF BB, platelet-derived growth factor BB; PKA, protein kinase A; PKC, protein kinase C; RACK1, receptor for activated protein kinase C; SARA, SMAD anchor for receptor activation; SD agar, synthetic drop-out agar; SNAPIN, SNARE-associated protein; TGF-β, transforming growth factor β.

blocking solution for 1 h at room temperature. SuperSignal West Pico chemiluminescent substrate (Pierce) was used according to the manufacturer's instructions to detect proteins.

Yeast Two-Hybrid Assay. The MATCHMAKER GAL4 Two-Hybrid System 3 (Clontech) was used. The ST7 cytoplasmic bait plasmids were constructed using the pGBKT7 bait vector. To generate the bait plasmids, the appropriate region of ST7's cytoplasmic domain was amplified from pCMV-SPORT-ST7 using *Pfu* polymerase and the appropriate oligonucleotides. $ST7_{cyto1}$ contains residues 498−840; $ST7_{cyto2}$, residues 498−667; $ST7_{cyto3}$, residues 668−840; $ST7_{cyto4}$, residues 498−625; $ST7_{cyto5}$, residues 498−560; and $ST7_{cyto6}$, residues 561−667. The purified PCR products (QIAquick spin PCR purification kit, Qiagen) were digested with restriction endonucleases *Eco*RI and *Xho*I and subcloned into *Eco*RI and *Sal*I sites of the bait vector pGBKT7. The *Saccharomyces cerevisiae* strain AH109, which contains *HIS3*, *ADE2*, and *MEL1* reporter genes, was transformed with the bait plasmid using the lithium acetate method described in the MATCHMAKER instruction manual (Clontech). Transformants containing the bait plasmid were selected by plating the cells on minimal SD agar lacking tryptophan (SD/-trp). A MATCHMAKER skeletal muscle cDNA library (Clontech) was amplified following the standard semisolid amplification procedure described in the MATCHMAKER instruction manual, and plasmid DNA was prepared using the QIAGEN plasmid Giga kit. To detect ST7-interacting proteins, AH109-$ST7_{cyto1}$ cells were transformed with the amplified library. Transformants were plated onto medium-stringency SD/-leu/-trp/-his agar. After incubation at 30 °C for several days, colonies were streaked onto SD/-leu/-trp and SD/-leu/-trp/-his agar plates. These yeast colonies were subjected to a higher stringency test (i.e., they were replica plated onto SD/-leu/-trp/-his/-ade agar plates). The colonies judged to grow well at high stringency conditions were restreaked for further analysis. Plasmid DNA was isolated from yeast colonies using the Zymoprep yeast plasmid miniprep kit (Zymo Research). Prey plasmids were rescued by transforming *E. coli* DH5α with the plasmid DNA isolated from yeast and by selecting these transformants on LB agar containing ampicillin at 100 μg/mL. The prey plasmids isolated from *E. coli* (QIAprep spin plasmid DNA miniprep kit, Qiagen) were sequenced. To map various binding domains in the ST7 cytoplasmic domain, bait plasmids encoding truncated forms of this domain ($ST7_{cyto2}$−$ST7_{cyto6}$) were engineered, and AH109 strains expressing the truncated bait proteins were transformed with the pACT2 prey plasmids isolated in the yeast two-hybrid screen. As a negative control, these strains were also transformed with a prey plasmid encoding the SV40 large T-antigen. To assess the specificity of the interaction between the prey proteins and ST7, a nonrelated bait protein, p53, was also tested for its interaction with the preys. The p53 bait plasmid, pGBKT7-p53, was included in the MATCHMAKER kit. All transformants were plated on quadruple drop-out agar (SD/-leu/-trp/-his/-ade). Growth on this medium indicated that the bait proteins tested interacted with the prey protein of interest.

Oligonucleotides. Primer sequences (5′-3′) used to construct the plasmids for the yeast two-hybrid screen and for co-immunoprecipitation studies were as follows. Restriction sites used for cloning are in boldface type, stop codons are in italics, and template sequences are underlined: 5′ primer for $ST7_{cyto1}$, $ST7_{cyto2}$, $ST7_{cyto4}$, and $ST7_{cyto5}$, CG**GAATTC**AAGCTTTATTCTCTGAGA; 3′ primer for $ST7_{cyto1}$ and $ST7_{cyto3}$, CG**CTCGAG**CTAACAAAGTAACAAAGCCTC; 5′ primer for $ST7_{cyto3}$, CG**GAATTC**GCGACAGTAGGAGCATGT; 3′ primer for $ST7_{cyto2}$ and $ST7_{cyto6}$, CG**CTCGAG***TTA*TTCCACTGCCGTTGTGGG; 3′ primer for $ST7_{cyto4}$, CG**CTCGAG***TTA*GTGAGTATGATTTCT; 3′ primer for $ST7_{cyto5}$, CG**CTCGAG***TTA*CCTCAGATTTTCCAA; and 5′ primer for $ST7_{cyto6}$, CG**GAATTC**CTAGCGGTACGATCT. The primer sequences (5′-3′) for subcloning HA-tagged partial prey proteins into pcDNA6-V5/His were as follows: 5′ primer AA**GCGGCCGC**GCCACCATGGCTTACCCATACGAT and 3′ primer CG**ACTAGT**GAGATGG TGCACGATGCACAGTTG or CG**TCTAGA**GAGATGGTGCACGATGCACAGTTG. Primer sequences for cloning full-length myotilin cDNA into the prey plasmid pACT2 were 5′ primer, CG**GAATTC**TAAGCATGTTTAACTACGAACGT and 3′ primer, CG**CTCGAG**TTAAAGTTCTTCACTTTCATAG. Primer sequences for isolating full-length RACK1 cDNA were 5′ primer, AA**GATATC**CATGACTGAGCAGATGACC and 3′ primer, AA**GTCGAC***CTAG CGTGTGCCA ATGGTCAC*. Primer sequences for isolating full-length MIBP cDNA were 5′ primer, AA**GATATC**CATGAAGCTCATCGTGGGC and 3′ primer AA**GTCGAC**TCACATGCTGTCCTGCTGGGA. Primer sequences for constructing pcDNA6-ST7-V5/His, pcDNA6-$ST7_{tr1}$-V5/His, and pcDNA6-$ST7_{tr2}$-V5/His: 5′ primer, which hybridizes to pCMV-SPORT vector sequence upstream of an *Eco*RI site and the *ST7* start codon, TAGGTGACAC TATAGAAGGTACGCCTGCAG; 3′ for ST7-V5/His, CG**GAATTC**TCGTAC CAAACAAAGTAACAAAGC; 3′ primer for $ST7_{tr1}$-V5/His, CG**CTCGAG**TCTTTCAAACAT TCTCAG; and 3′ primer for $ST7_{tr2}$-V5/His, CG**CTCGAG**CTTACAAGTACATCCCAA.

Construction of Mammalian Expression Plasmids. cDNAs encoding the prey proteins of interest were PCR amplified from the appropriate pACT2 prey plasmids using *Pfu* polymerase. The 5′ primer used hybridizes with the pACT2 HA epitope sequence located upstream of the cDNA insertion site; the 3′ primer used hybridizes with sequence on pACT2 downstream of the cDNA insertion site. Therefore, each PCR product contains the entire partial prey cDNA with an N-terminal HA-tag. The GAL4 activation domain was not amplified in this procedure. PCR products (QIAquick spin PCR purification kit, Qiagen) were digested with *Spe*I or *Xba*I, depending upon which 3′ primer was used, and subcloned into the *Eco*RV and *Xba*I sites of the mammalian expression vector pcDNA6-V5/HisA (Invitrogen). Each PCR product contains a stop codon so that the proteins would not be V5/His tagged. Any full-length cDNA inserts isolated from the yeast library were used to generate an expression plasmid containing the entire open reading frame with an N-terminal HA tag. First, the entire open reading frame was amplified from the pACT2 plasmid containing the ORF using *Pfu* polymerase. The purified PCR product was digested with *Eco*RI and *Xho*I and subcloned into the corresponding sites in pACT2. The HA-tagged, full-length prey protein cDNA was amplified from this plasmid and subcloned into pcDNA6-V5/His in the same manner as the others. Additional full-length cDNAs were amplified from the MATCHMAKER skeletal muscle cDNA library using *Pfu* polymerase and the

Table 1: Structure of the *ST7* Gene

exon	intron/exon boundaries		exon (bp)	exon/intron boundaries		intron (kb)
1			79	GGGGTGTACG	gtaagtgtcc	55.9
2	ttaattttag	GAAATGGTGC	57	GTGTCAACTG	gtaagtcatt	22.8
3	tatcttccag	CTTGTGGAGA	136	TACTATAAGG	gtaattctac	9.4
4	ttttttttcag	TTTTCAGGAT	203	TATTTTTCAG	gtgtgttttt	12.4
5	atcttcacag	GGAAATCTGA	1105	TTGAAAGAAG	gtcagtatca	1.8
6	ctctcaaaag	ATCATTTGAA	133	ACCTAATCAG	gtatattgca	3.5
7	atttttgtag	GCTTCTGTTT	866	ACTTTGTTAG		

appropriate primers. The purified PCR products were digested with *Eco*RV and *Sal*I and subcloned into the *Eco*RV and *Xho*I sites of pcDNA6-HA, which was constructed by excising the HA epitope from pcDNA6-HA-MIBP$_p$ using *Eco*RI and subcloning the epitope into the *Eco*RI site of pcDNA6-V5/His. Again, because the primers were designed to contain the endogenous stop codons, these proteins were not tagged by V5/His. To construct mammalian expression plasmids containing full-length V5/His tagged ST7 or truncated V5/His tagged ST7, the appropriate region of ST7 was amplified from pCMV-SPORT-ST7 using *Pfu* polymerase and the appropriate oligonucleotides. The PCR products purified by a QIAquick spin PCR purification kit were digested with restriction endonucleases *Eco*RI (ST7) or with *Eco*RI and *Xho*I (ST7$_{tr1}$ and ST7$_{tr2}$) and subcloned into *Eco*RI or *Eco*RI and *Xho*I sites in pcDNA6-V5/HisA from Invitrogen. Elimination of the endogenous stop codons caused the proteins encoded by these cDNAs to have C-terminal V5 and His epitope tags.

Co-Immunoprecipitation of Proteins from Transiently Transfected 293-T Cells. 293-T cells were plated in 60-mm diameter tissue culture dishes (1.5×10^6 cells per dish) 1 day prior to transfection. Cells were transfected with a total of 10 μg of plasmid DNA using LipofectAMINE (Invitrogen) following the manufacturer's instructions. Forty-eight h after transfection, the cells were washed once in cold PBS and collected in cold lysis buffer (50 mM Tris-HCl, pH 7.2, 150 mM NaCl, 0.5% NP-40, 50 mM NaF, 1 mM Na_3VO_4, 1 mM benzamidine, 1 mM phenylmethylsulfonyl fluoride, 25 μg/mL aprotinin, and 25 μg/mL leupeptin). The cells were incubated in the lysis buffer for 30 min on ice with periodic gentle vortexing. The protein extracts were clarified by centrifugation (25 000*g*) for 30 min at 4 °C. The supernatants were transferred to fresh tubes and centrifuged (25 000*g*) for an additional hour at 4 °C. Total protein concentration was determined using the Coomassie protein assay reagent (Pierce) following the manufacturer's instructions. For immunoprecipitation, protein extracts (250 or 500 μg) were diluted in buffer containing 25 mM Tris-HCl, pH 7.4, 30 mM $MgCl_2$, 40 mM NaCl, 0.5% NP-40 and precleared using normal rabbit serum (0.5 μg) (Santa Cruz Biotechnology) and protein A-agarose beads (20 μL) (Santa Cruz Biotechnology) for 30 min at 4 °C with end-over-end mixing. The precleared supernatants were incubated with 2 μg of rabbit polyclonal anti-HA antibody (Y-11, Santa Cruz Biotechnology) for 2 h at 4 °C with end-over-end mixing. A control reaction was carried out for each protein pair in which no HA antibody was included in the immunoprecipitation reaction. Protein A-agarose beads (20 μL) were added, and the reactions were incubated for an additional hour at 4 °C with end-over-end mixing. The agarose pellets were washed three times with a buffer containing 25 mM Tris-HCl, pH 7.4, 30 mM $MgCl_2$, 40 mM NaCl, 1.0% NP-40 and once with a buffer containing 25 mM Tris-HCl, pH 7.4, 30 mM $MgCl_2$, 40 mM NaCl. Following the washes, the pellets were resuspended in 40 μL of 1X Laemelli SDS−PAGE sample buffer. Denatured immunoprecipitated proteins were separated by SDS−PAGE and transferred to Immobilon-P membrane. Such membranes were blocked for 2 h in blocking solution. Blocked membranes were incubated with a monoclonal V5 antibody and a monoclonal HA antibody (F-7, Santa Cruz Biotechnology) diluted in the blocking solution for at least 2 h at room temperature and with the appropriate horseradish peroxidase-conjugated secondary antibody diluted in blocking solution for 1 h at room temperature. SuperSignal West Pico chemiluminescent substrate was used to detect proteins.

RESULTS

Isolation of ST7 cDNA from a Human Heart Muscle cDNA Library. Because the *ST7* cDNA fragments originally isolated had been obtained from multiple cDNA libraries using PCR with relatively low fidelity DNA polymerases (*2*), there was a possibility that they contained PCR-generated mutations. Therefore, we isolated *ST7* cDNA from a human heart cDNA library using the GeneTrapper cDNA Positive Selection System. Comparison of this DNA sequence to the two isoforms found by Qing et al. (*2*) revealed that this *ST7* cDNA was the shorter of the two. It lacks 57 nucleotides at its 5′ end (nucleotides 79−136 of GenBank accession number NM_013437). To determine whether this isoform could be the product of alternative splicing of the transcript, we used the human genome BLAST program to search the human genomic DNA database for the *ST7* sequence. The *ST7* gene was localized to an ~100 kb region of human chromosome 8q (Locus Link ID 29967). This confirmed the fluorescent in situ hybridization data of Qing et al. (*2*) showing ST7's location to be chromosome 8q22.2−23.1. The sequence contains seven putative exons (Table 1). The 57 nucleotides missing in the short isoform correspond to the second exon, indicating that it may be the product of alternative splicing of the transcript.

ST7 Is a Novel LDLR-Related Protein. The similarity between ST7 and LRP3 strongly suggested that ST7 is a novel LRP. Comparison of residues 27−604 of ST7 with residues 42−627 of LRP3 using BLAST revealed that the two proteins are 50% identical and 66% similar. After this research had been carried out, Sugiyama et al. (*10*) reported the discovery of a murine LDLR-related protein, LRP9, which closely resembles ST7 and LRP3. They suggested that LRP9, LRP3, and ST7 constitute a novel subfamily of the LDLR superfamily. Comparison of ST7 with residues 28−698 of murine LRP9 showed that the proteins are 35% identical and 46% similar. The most striking characteristics

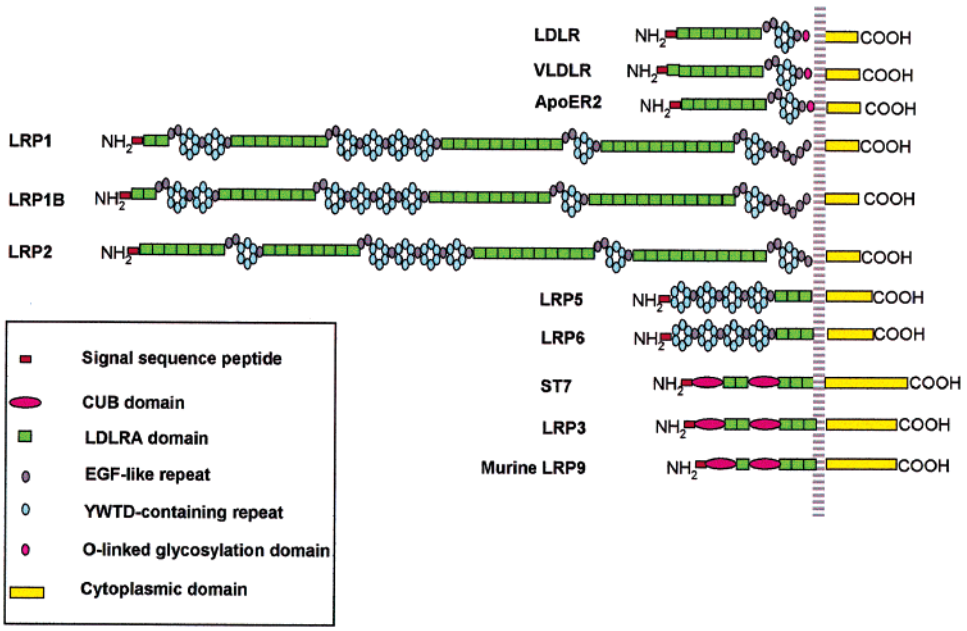

FIGURE 1: Structures of representative proteins of the LDLR superfamily (adapted from ref *6*). The types of domains in these proteins and the organization of these domains divide the superfamily into at least four subfamilies: (1) LDLR, VLDLR, and ApoER2; (2) LRP1, LRP1B, and LRP2; (3) LRP5 and LRP6; and (4) ST7, LRP3, and murine LRP9. The cytoplasmic domains of these proteins contain motifs implicated in endocytosis and/or signal transduction, which are not shown.

```
ST7         498 KLYSLRMFERRSFETQLSRVEAELLRREAPPSYGQLIAQGLIPPVEDFPVCSPNQASVLE
LRP3        521 KLYSLRTQEYRAFETQMTRLEAEFVRREAPPSYGQLIAQGLIPPVEDFPVYSASQASVLQ
LRP9        446 KLYAIRTQEYSIFAP-LSRMEAEIVQQQAPPSYGQLIAQGAIPPVEDFPTENPNDNSVLG
consensus       KLYslRtqEyr FetqlsRvEAElvrreAPPSYGQLIAQGlIPPVEDFPv spnqaSVL

ST7         558 NLR--LAVRSQLG-FTSVRLPMAGRSSNIWNRIFNFARSRHSGSLALVSADGDEVVPSQS
LRP3        581 NLR--TAMRRQMRRHASRRGPSRRRLGRLWNRLFHRPRAPR-GQIPLLTAAR----PSQ-
LRP9        525 NLRSLLQILRQDMTPGGTSGGRRRQRGRSVRRLVRRLR--RWGLLPRTNT------PAR-
consensus       NLR  lavrrQl   as rgp rrr griwnRlfhr R  r G lplvsa      Psq

ST7         615 TSREPERNHTHRSLFSVESDDTDTENERRDMAGASGGVAAPLPQKVPPTTAVEATVGACA
LRP3        633 ----------------TVLGDGFLQP--------APG--AAPD----PPAPLMD--TG---
LRP9        576 -------------------APETRSQ-------------VTPS----VPSEALDDSTG---
consensus                     sv gddt t          a g  aaP     pPt avd ttG

ST7         675 SSSTQSTRGGHADNGRDVTSVEPPSVSPARHQLTSALSRMTQGLRWVRFTLGRSSSLSQN
LRP3        659 -----STR---AAGDR------PPS-AP-----------------------GRAPEVGPS
LRP9        598 ----HACEGG-AVGGQDGEQ-APP--LP-----------------------IKTPIPTPS
consensus           strgg A ggrd     PPs  P                       grsp lsps

ST7         735 QSPLRQLDNGVSGREDDDDVEMLIPISDGSSDFDVNDCSRPLLDLASDQGQGLRQPYNAT
LRP3        681 GPPLP------SGLRDPE---CR-PV------DKDRKVCREPLADGPAP-ADAPREPCSAQ
LRP9        627 TLPALA-----TVSETPG------PL------PSVPVESS-LLSGVVQVLRGRLLP-SLW
consensus         Pl       sg edpd      Pi     d dv vcs pLldg    g g r P sa

ST7         795 NPG------VRPSNRDGPCERCGIVHTAQIPDTCLEVTLKNETSDDEALLLC
LRP3        725 DPHP---QVSTASSTLGPHSPEPLGVCRNPPPPCSPML---EASDDEALLVC
LRP9        668 SPGPTWTQTGTHTTVLSPEDEDDVLLLP-LAEPEVWVV---EA-EDEPLLA-
consensus         Pgp   q  t ss lgP e e ivv  qipdpcl vl   EasdDEaLLlc
```

FIGURE 2: Alignment of the cytoplasmic domains of ST7, LRP3, and murine LRP9. Regions of identity in these proteins are red, and regions of similarity are blue. The consensus sequence is shown beneath the alignment in black. Uppercase letters designate amino acids conserved in all three proteins. Lowercase letters designate amino acids conserved in two of the three proteins. Note the high degree of sequence conservation in the juxtamembrane region (498−560 of ST7) and in the extreme carboxy terminal region of these proteins.

common to all three proteins are that (1) their extracellular domains contain the same types of functional domains arranged in an identical configuration (Figure 1); (2) the juxtamembrane regions of their cytoplasmic domains are highly conserved (Figure 2), strongly suggesting that this region is functionally important; and (3) their cytoplasmic tails contain putative signals for endocytosis and sequences that may participate in signal transduction (Figure 3). These

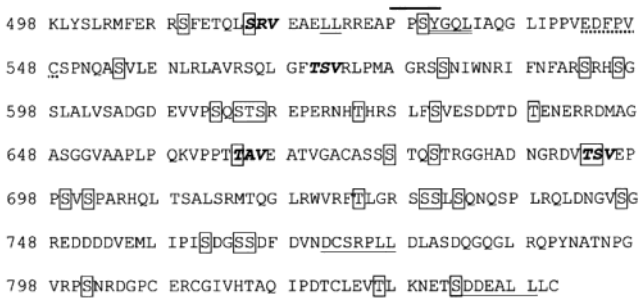

FIGURE 3: Putative endocytic and signal transduction motifs identified in ST7's cytoplasmic domain. The YXXø internalization motif is indicated by a double underline. The NPXY-like internalization motif is shown by a dotted underline. A single underline denotes the three dileucine motifs. Potential phosphorylation sites are boxed. The four PDZ domain binding motifs are shown in boldface italic font. A line is drawn above the WW domain binding motif.

highly related features are strong evidence that ST7, LRP3, and LRP9 comprise an LDLR subfamily.

Analysis of the ST7 Protein. Qing et al. (*2*) predicted that *ST7* encodes a type I single-pass transmembrane protein. To gain additional information regarding ST7's protein structure, its sequence was further analyzed using proteomic analysis tools available through the ExPASy Molecular Biology Server (www.expasy.ch). The protein's putative extracellular domain, residues 1−473, contains a signal sequence peptide motif (residues 1−27) as determined by the SignalP prediction program (*11*). Such motifs are characteristic of proteins targeted to the plasma membrane (*12*). This region also contains five LDLRA domains arranged in two clusters and two CUB domains, as determined using ScanProsite (*13*) (Figure 1). The first LDLRA cluster contains two domains (146−182 and 195−236), and the second cluster contains three domains (355−392, 393−430, and 431−467). Each LDLRA domain consists of ∼40 residues, with six conserved cysteine residues that form three intramolecular disulfide bonds and with conserved serine, aspartic acid, and glutamic acid residues at the domain's C-terminus (*14*). All of the members of the LDLR superfamily contain LDLRA domain repeats (*5*, *6*). In many of these proteins, such domains have been demonstrated to function as ligand binding sites (*14*). A single CUB domain (residues 28−140 and 240−353) precedes each LDLRA domain cluster (Figure 1). This feature is unique to the LDLR subfamily consisting of ST7, LRP3, and LRP9. CUB domains are composed of ∼110 amino acids with four conserved cysteine residues that form two intramolecular disulfide bonds and are believed to participate in protein−protein interactions (reviewed in refs *15* and *16*). Exon 2 of *ST7*, which is lacking in the isoform used in our studies, encodes the protein sequence between the signal sequence peptide and the first CUB domain. Therefore, loss of this exon's sequence does not affect any of the functional domains present in ST7's extracellular domain. The other ST7 isoform simply contains 19 additional amino acids immediately upstream of the first CUB domain.

The putative extracellular domain of ST7 is followed by a single hydrophobic transmembrane helix flanked by positively charged residues (residues 474−497) (*2*). The C-terminal cytoplasmic tail of the protein (residues 498−840) contains several sequence motifs related to endocytosis (Figure 3). These endocytic signaling motifs include an YXXø motif (YGQL, 530−533), a NPXY-like motif (EDFPVC, 543−548), and three potential dileucine repeats (521−522, 776−777, and 837−839). In these consensus sequences, X represents virtually any amino acid, and ø represents any amino acid with a bulky hydrophobic group (endocytic signals reviewed in ref *17*). Several putative signaling motifs were also found. Four PDZ domain binding motifs, (S/T)XV (SRV, 515−517; TSV, 570−572; TAV, 664−666; and TSV, 693−995), and a WW domain binding motif, PPXY (PPSY, 527−530), are present (Figure 3). Moreover, the cytoplasmic domain of ST7 is notably rich in proline, serine, and threonine residues. Proline-rich regions are often involved in protein−protein interactions (*18*). Because the phosphorylation of residues in the tails of receptors can regulate their interactions with intracellular proteins, we analyzed the cytoplasmic tail of ST7 for putative serine, threonine, and tyrosine phosphorylation sites using NetPhos 2.0 prediction software (*19*). Twenty-five serines and seven threonines were predicted to be potential sites of phosphorylation (based on a score of ∼0.5 or greater) (Figure 3). Six of the 32 putative phosphorylation sites, three serines and three threonines, are located within the consensus sequence for phosphorylation by PKC (Table 2). Eight sites, five serines and three threonines, are located within the consensus sequence for phosphorylation by PKA (Table 2). Serine and threonine residues constituting three of the four PDZ domain binding motifs, as well as the serine residue present in the WW domain binding motif, were also predicted to be potential phosphorylation sites. The three tyrosines present in ST7's cytoplasmic domain were not predicted to be phosphorylated. However, one of these tyrosine residues is shared by the WW domain-binding motif and the YXXø internalization motif (*PPS*-**Y**-GQL), and several groups have reported phosphorylation of tyrosines in the context of either motif (*20*−*22*).

Table 2: Putative PKC and PKA Phosphorylation Sites in ST7's Cytoplasmic Domain

position	sequence	kinase
509	FERRSFETQ	PKA
581	AGRSSNIWN	PKA
596	RSRHSGSLA	PKA
615	PSQSTSREP	PKC
624	ERNHTHRSL	PKA, PKC
680	SSTQSTRGG	PKC
693	GRDVTSVEP	PKA
724	WVRFTLGRS	PKA
730	GRSSSLSQN	PKA
746	DNGVSGRED	PKC
801	GVRPSNRDG	PKA, PKC
826	CLEVTLKNE	PKC

Plasma Membrane Localization of ST7-V5/His. To determine whether ST7 localizes to cellular membranes, as predicted by our analysis of the structure of ST7 protein, we isolated plasma membrane-enriched and soluble fractions from SHAC cells transfected with a plasmid encoding V5/His epitope tagged ST7 or with the empty plasmid (vector-transfected control). The fractions were analyzed by Western blotting using the anti-V5 antibody. ST7-V5/His was detected in the appropriate plasma membrane-enriched fraction and was not in the matching soluble fraction, indicating that V5/His tagged ST7 localizes to the plasma membrane (Figure 4). As a control, we also analyzed these fractions by blotting with an antibody against Na^+/K^+ ATPase, an integral

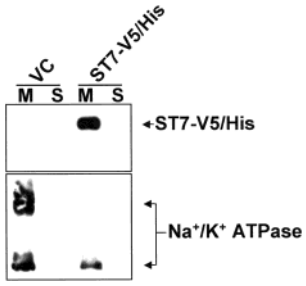

FIGURE 4: V5/His tagged ST7 protein encoded by the transfected plasmid is localized in the membrane of the SHAC cell recipients. Plasma membrane-enriched (M) and soluble, cytosolic (S) fractions were isolated from a vector control transfected SHAC cell strain (lanes 1 and 2) and from a transfectant overexpressing full-length ST7 (lanes 3 and 4). A total of 20 μg of each fraction was separated in a 10% SDS−polyacrylamide gel, transferred to PVDF membrane, and probed with anti-V5 antibody (upper panel) and an antibody specific for a membrane protein, that is, anti-Na^+/K^+ ATPase antibody (lower panel). The latter protein has multiple isoforms.

membrane protein. As expected, this latter protein was detected in the plasma membrane-enriched fractions and was not in the soluble fractions.

Identification of Proteins that Interact with the Cytoplasmic Domain of the ST7 Protein. Tumorigenicity studies recently conducted in this laboratory strongly suggest a functional role for ST7's cytoplasmic tail in inhibiting tumor formation (data to be published elsewhere). Because of this finding and because our analysis of ST7's cytoplasmic domain revealed several potential endocytic and signal transduction motifs, we chose to identify proteins that interact with ST7's cytoplasmic C-terminus, using the yeast two-hybrid system (described in detail under Experimental Procedures). More than 30 different ST7-interacting cDNAs were identified. Of these, six cDNAs, encoding proteins of the greatest interest, were chosen for further study. These are (1) RACK1, a WD domain-containing protein implicated as a key cellular scaffold protein that interacts with multiple cellular receptors (*23*−*25*); (2) MIBP, an integrin binding protein believed to participate in signal transduction pathways regulating myogenesis (*26*); (3) SARA, a FYVE domain-containing cellular scaffold protein that shuttles SMAD2 and SMAD3 to the cytoplasmic domains of TGFβ receptors (*27*) [recent studies also implicate SARA in the Rab5-mediated endocytic pathway (*28*)]; (4) α-actinin-2, a cytoskeletal protein considered to link plasma membrane receptors to the cytoskeleton (*29*); (5) myotilin, a novel cytoskeletal protein that interacts with α-actinin-2 [defects in myotilin cause limb-girdle muscular dystrophy type 1A (*30*−*32*)]; and (6) SNAPIN, a novel binding partner for the SNAP-25 component of the SNARE vesicular transport complex (*33*). To verify that these six cDNAs encode the proteins responsible for the interactions we observed in our yeast two-hybrid screen, AH109 yeast cells containing the $ST7_{cyto1}$ bait plasmid were transformed with each of the six prey plasmids, and the transformants were plated on selection medium. Each of the proteins tested interacted with the cytoplasmic domain of ST7, as detected by reporter gene activity.

Polymerase chain reaction (PCR) was used to subclone each of the six prey cDNAs into mammalian expression vector pcDNA6-V5/His. An N-terminal HA-epitope tag was included to facilitate detection of the proteins, and a stop codon was included at the 3′ end of each cDNA to exclude the V5 and His epitope tags from the resulting proteins. Table 3 indicates the cDNAs isolated from yeast. Those encoding only a portion of the prey protein are designated by a subscript p. Because three of the four myotilin cDNAs isolated from yeast contained the entire open reading frame and some 5′ upstream untranslated sequence, the entire myotilin open reading frame was subcloned into the expression vector. Sequencing of each insert to verify the fidelity of the PCR reactions revealed that we had isolated the longer isoform of the *MIBP* cDNA (GenBank accession number AK001663), which contains a 132-nucleotide in-frame insertion between nucleotides 328 and 329 of the shorter *MIBP* coding sequence (GenBank accession number NM_014446). The sequences of the two MIBP proteins are identical except for an additional 44 residues in the longer form. Sequencing also demonstrated that a variant *SARA* cDNA had been isolated. To date, three *SARA* transcript variants have been observed and are reported in GenBank. Our partial cDNA, which lacks the 81 nucleotides of exon 14, represents a fourth *SARA* transcript variant.

Table 3: Identification of Proteins that Interact with the Cytoplasmic Domain of ST7[a]

name	clones isolated	ind. clones isolated	prey protein size	function/pathway
$MIBP_p$	1	1	92-COOH	signal transduction
$RACK1_p$	2	2	65-COOH 106-COOH	signal transduction
$SARA_p$	1	1	731-COOH	signal transduction
myotilin	4	2	5′UTR-COOH 250-COOH	actin cytoskeleton
α-actinin-2_p	1	1	307-COOH	actin cytoskeleton
$SNAPIN_p$	2	1	17-COOH	synaptic transmission

[a] To identify ST7-interacting proteins, the complete ST7 cytoplasmic domain was used as bait in a yeast two-hybrid screen of a human skeletal muscle cDNA library. The majority of positive cDNAs identified encode a partial prey protein, designated by a subscript p. Column four lists the region of each prey protein encoded by isolated cDNAs. Three of the four myotilin prey plasmids isolated contained a cDNA that includes the entire open reading frame and some of the 5′ untranslated sequence (5′UTR).

Confirmation of the Protein−*Protein Interactions within Human Cells.* Protein−protein interactions identified using the yeast two-hybrid assay are considered valid only if verified by other biochemical methods. Therefore, we used co-immunoprecipitation to determine whether the six prey proteins identified interact with ST7's cytoplasmic domain in human cells. HEK293-T cells were transiently cotransfected with plasmids encoding an HA-tagged partial prey protein and ST7-V5/His protein, and the HA-tagged prey protein was immunoprecipitated from lysates of these cells. The immunoprecipitation products were analyzed by Western blotting with a monoclonal V5 antibody to detect ST7-V5/His and a monoclonal HA antibody to detect the HA-tagged prey proteins. The ST7-V5/His protein was co-immunoprecipitated with HA-$RACK1_p$ (Figure 5A), HA-$MIBP_p$ (Figure 5B), and HA-$SARA_p$ (Figure 5C), indicating an interaction between these protein pairs. ST7-V5/His failed to co-immunoprecipitate with HA-α-$actinin2_p$, HA-$SNAPIN_p$, and HA-myotilin. An example is shown in Figure 5D. Failure to detect an interaction between these three prey proteins and ST7-V5/His by co-immunoprecipitation does not exclude these as ST7-interacting proteins because the

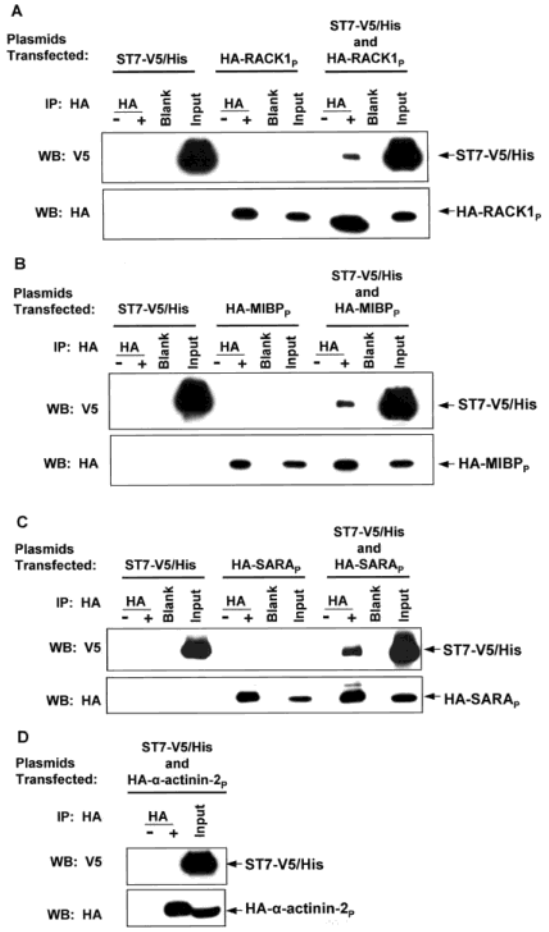

FIGURE 5: ST7 interacts with $RACK1_p$, $MIBP_p$, and $SARA_p$ in human cells. (A) Western blotting analysis of HA immunoprecipitation reactions from 293-T cells transiently transfected with ST7-V5/His, HA-$RACK_p$, or both ST7-V5/His and HA-$RACK_p$. The upper panel was probed with anti-V5 antibody; the lower panel was probed with anti-HA antibody. Lanes designated with a minus (−) sign contain negative control IP reactions (i.e., immunoprecipitation reactions without HA antibody); lanes designated with a plus (+) sign contain immunoprecipitation reactions with anti-HA; lanes designated as input contain 25 μg of the lysate used in the immunoprecipitation reactions; and lanes designated as blank were not loaded. (B) Same as panel A except cells were transfected with ST7-V5/His, HA-$MIBP_p$, or both ST7-V5/His and HA-$MIBP_p$. (C) Same as panel A except cells were transfected with ST7-V5/His, HA-$SARA_p$, or both ST7-V5/His and HA-$SARA_p$. (D) Same as panel A except cells were transfected with both ST7-V5/His and HA-α-actinin-2_p.

co-immunoprecipitation approach is less sensitive than the yeast two-hybrid assay. The interaction of these proteins with ST7 may simply have been missed as the result of being weaker or transient.

Whether full-length RACK1 and MIBP proteins interact with ST7 was determined as follows. cDNAs encoding full-length RACK1 and MIBP were isolated from the MATCHMAKER skeletal muscle cDNA library using PCR with appropriate oligonucleotides and subcloned into pcDNA6-HA. The endogenous stop codon was retained in each full-length cDNA so that the resulting proteins would not be tagged by the V5 and His epitopes. We sequenced the *HA-RACK1* and *HA-MIBP* cDNA inserts and verified that the PCR reactions were faithful. 293-T cells were transiently cotransfected with plasmids encoding HA-RACK1 or HA-MIBP and ST7-V5/His, and the HA-RACK1 or HA-MIBP

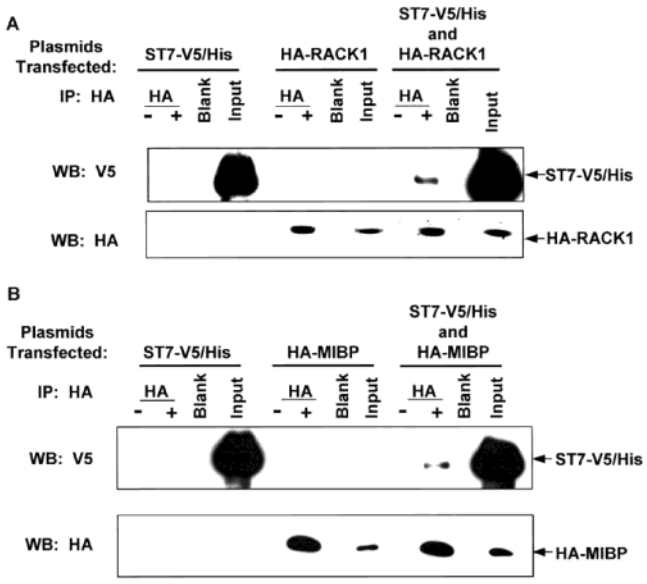

FIGURE 6: ST7 interacts with full-length RACK1 and MIBP in human cells. (A) Western blotting analysis of HA immunoprecipitation reactions from 293-T cells transiently transfected with ST7-V5/His, HA-RACK, or both ST7-V5/His and HA-RACK. The upper panel was probed with anti-V5 antibody; the lower panel was probed with anti-HA antibody. Lanes designated with a minus (−) sign contain negative control IP reactions (i.e., immunoprecipitation reactions without HA antibody); lanes designated with a plus (+) sign contain immunoprecipitation reactions with anti-HA; lanes designated as input contain 25 μg of the lysate used in the immunoprecipitation reactions; and lanes designated as blank were not loaded. (B) Same as panel A except cells were transfected with ST7-V5/His, HA-MIBP, or both ST7-V5/His and HA-MIBP.

protein was immunoprecipitated from lysates of these cells. The immunoprecipitation products were analyzed by Western blotting with a monoclonal V5 antibody and a monoclonal HA antibody. ST7-V5/His was co-immunoprecipitated with both HA-RACK1 (Figure 6A) and HA-MIBP (Figure 6B), indicating that the full-length RACK1 and MIBP proteins interact with ST7. The ability of full-length SARA to interact with ST7 has not yet been determined because we were unable to amplify a cDNA containing the full-length variant *SARA* using PCR.

Identification of the RACK1, MIBP, and SARA Binding Domains within ST7's Cytoplasmic Domain. To identify the specific region within ST7's cytoplasmic domain required for its interaction with RACK1, MIBP, and SARA, we used the yeast two-hybrid assay with truncated forms of the ST7 cytoplasmic domain as bait (Figure 7). AH109 strains expressing the truncated $ST7_{cyto}$ bait proteins were transformed with the pACT2 prey plasmids isolated in the yeast two-hybrid screen. As a negative control, we transformed these AH109 strains with a prey plasmid encoding the SV40 large T-antigen, which does not interact with ST7. To assess the specificity of the interaction between the prey proteins and the ST7 bait proteins, we also tested a nonrelated bait protein, p53, for its ability to interact with RACK1, MIBP, and SARA. Transformants were plated on selective agar (SD/-leu/-trp/-his/-ade). Failure of the transformants to grow indicated that the truncated $ST7_{cyto}$ bait protein or the p53 bait protein failed to bind to the prey protein. Table 4 summarizes the results of these studies.

As previously determined, the $ST7_{cyto1}$ bait protein (residues 498−840) was able to interact with RACK1, MIBP,

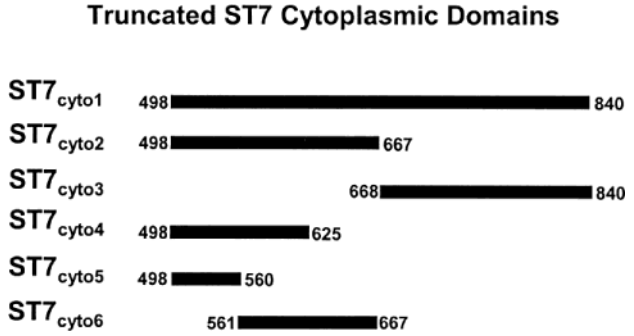

FIGURE 7: Illustration of the truncated ST7 cytoplasmic domain bait proteins used to determine the location of the MIBP, SARA, and RACK1 binding sites in ST7. The appropriate bait-containing AH109 strains were transformed with an $MIBP_p$, $SARA_p$, or $RACK1_p$ prey plasmid. As a negative control, the bait-containing AH109 strains were also transformed with a prey plasmid encoding the SV40 large T-antigen, which does not bind to ST7. Transformants were plated on the most stringent medium, SD/-trp/-leu/-his/-ade. Growth on this medium indicated that the bait and prey proteins tested were able to interact within yeast cells.

Table 4: Interaction of Prey Proteins with Truncated ST7 Bait Proteins[a]

PREY BAIT	$MIBP_p$	$SARA_p$	$RACK1_p$	SV40 T-Ag
$ST7_{cyto1}$	+	+	+	−
$ST7_{cyto2}$	+	+	+	−
$ST7_{cyto3}$	NA	NA	NA	NA
$ST7_{cyto4}$	+	+	+	−
$ST7_{cyto5}$	+	+	+	−
$ST7_{cyto6}$	−	−	+	−
p53	−	−	−	+

[a] Full-length and truncated ST7 cytoplasmic domains (shown in Figure 7) were used as bait to identify the MIBP, SARA, and RACK1 binding sites in ST7. SV40 large T-antigen (SV40 T-Ag), which does not interact with ST7's cytoplasmic domain, served as the negative control. To assess the specificity of the interaction between the prey proteins and ST7, a nonrelated bait protein, p53, was tested for its interaction with the preys. Plus (+) signs indicate that a bait protein interacted with the prey protein tested; minus (−) signs indicate that these proteins did not interact. NA, not applicable because the $ST7_{cyto3}$ bait protein self-activated the yeast reporter genes.

and SARA but not with SV40 large T-antigen, the negative control. The $ST7_{cyto1}$ bait was divided into an N-terminal $ST7_{cyto2}$ fragment (residues 498−667) and a C-terminal $ST7_{cyto3}$ fragment (residues 668−840). RACK1, MIBP, and SARA interacted with $ST7_{cyto2}$; the negative control did not. When we tested the $ST7_{cyto3}$ fragment in the absence of prey, it activated reporter gene expression in AH109. Therefore, it was uninformative in these studies. Because our proteomic analysis of ST7 indicated that the juxtamembrane region of the cytoplasmic tail may constitute a functionally important domain, we further divided the N-terminal $ST7_{cyto2}$ fragment into three parts, $ST7_{cyto4}$ (residues 498−625), $ST7_{cyto5}$ (residues 498−560), and $ST7_{cyto6}$ (residues 561−625). The negative control did not interact with any of these fragments. RACK1, MIBP, and SARA each interacted with $ST7_{cyto4}$ and $ST7_{cyto5}$. Only RACK1 was able to interact with the $ST7_{cyto6}$. $ST7_{cyto6}$ lacks the highly conserved residues of the juxtamembrane region of ST7's cytoplasmic domain. These results demonstrate that the membrane-proximal 63 amino acids of ST7 contain the critical residues involved in its interaction with MIBP and SARA. Because RACK1 interacted with all

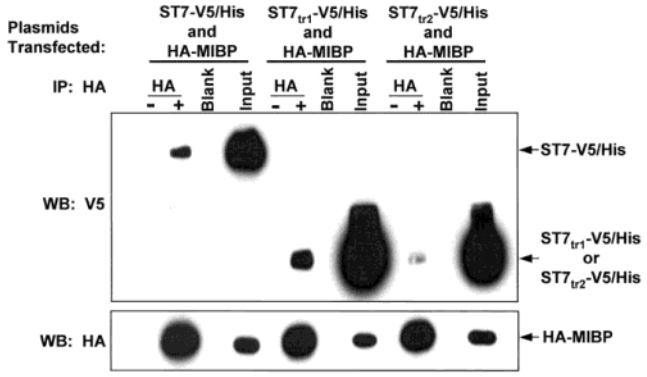

FIGURE 8: The first 10 amino acids of the ST7 cytoplasmic domain may suffice for MIBP binding. Western blotting analysis of HA immunoprecipitation reactions from 293-T cells transiently transfected with ST7-V5/His and HA-MIBP, $ST7_{tr1}$-V5/His and HA-MIBP, or $ST7_{tr2}$-V5/His and HA-MIBP. The upper panel was probed with anti-V5 antibody to detect both the full-length and the truncated V5-tagged ST7 proteins; the lower panel was probed with anti-HA antibody to detect HA-MIBP. Lanes designated with a minus (−) sign contain negative control IP reactions (i.e., immunoprecipitation reactions without HA antibody); lanes designated with a plus (+) sign contain immunoprecipitation reactions with anti-HA; lanes designated as input contain 25 μg of the lysate used in the immunoprecipitation reactions; and lanes designated as blank were not loaded.

of the bait proteins spanning residues 498−667, the critical residues for its interaction with ST7 must be contained in these truncated proteins. None of the prey proteins tested interacted with the nonrelated bait protein, p53, indicating that the interaction between the ST7 bait proteins and the prey proteins is likely to be specific. As expected, the SV40 large T-antigen prey protein interacted with p53.

Once the MIBP binding domain had been mapped to the membrane proximal region of ST7, co-immunoprecipitation studies using transiently cotransfected 293-T cells were carried out to determine whether this protein interacts with ST7 protein truncated within its juxtamembrane region. Two plasmids encoding a V5/His tagged truncated ST7 protein were used. Plasmid V5/His-tagged $ST7_{tr1}$ encodes a truncated protein (residues 1−507). It contains ST7's extracellular and transmembrane domains but only the first 10 residues of its 343 amino acid cytoplasmic domain. When tested, this truncated protein was shown to lack the ability to block tumor formation. Plasmid V5/His-tagged $ST7_{tr2}$ encodes a truncated protein (residues 1−498). It contains ST7's extracellular and transmembrane domains but only the first amino acid of its cytoplasmic domain. 293-T cells were transiently cotransfected with plasmids encoding HA-tagged full-length MIBP and ST7-V5/His, $ST7tr_1$-V5/His, or $ST7_{tr2}$-V5/His. HA-MIBP was immunoprecipitated from lysates of the transiently cotransfected cells. The immunoprecipitation products were analyzed by Western blotting with a monoclonal V5 antibody to detect V5-tagged ST7 proteins and a monoclonal HA antibody to detect HA-MIBP. Both ST7-V5/His and the $ST7_{tr1}$-V5/His were strongly co-immunoprecipitated with HA-MIBP (Figure 8), indicating an interaction between these protein pairs. Figure 8 shows that the $ST7_{tr2}$-V5/His protein was also co-immunoprecipitated with HA-MIBP, although to a much lesser extent. This was somewhat surprising.

DISCUSSION

On the basis of our analysis of the structure of ST7 protein, we conclude that it is a novel member of the LDLR superfamily, and in particular, is closely related to LRP3 and murine LRP9. The striking similarity between the structures of these three proteins (see Figures 1 and 2) indicates that they constitute a distinct LDLR subfamily, as first suggested by Sugiyama et al. (*10*). Therefore, ST7 should now be referred to as LRP12. ST7 contains four critical structural motifs linking it to this superfamily: (1) an N-terminal signal sequence; (2) multiple LDLRA domains arranged in clusters in the extracellular region of the protein; (3) a single transmembrane domain; and (4) a cytoplasmic tail containing motifs believed to function in endocytosis and/or signal transduction. The extracellular region of every LDLR superfamily protein contains various numbers of LDLRA domain repeats arranged in clusters, and these domains function in ligand binding (*5*, *6*, *14*). Unlike the prototypical members of the LDLR superfamily, ST7, LRP3, and murine LRP9 lack EGF-like repeats and YWTD-containing domains, and instead, contain CUB domains. The latter structures are found in a diverse array of functionally unrelated extracellular proteins (reviewed in ref *15*). For example, the peripheral membrane protein cubilin, anchored in the external side of the plasma membrane through its N-terminus, contains 27 extracellular CUB domains that function in ligand binding (reviewed in ref *16*). The LDLRA and CUB domains present in ST7 probably enable ST7 to bind to extracellular ligands. No ST7 ligands have yet been identified, but ongoing work in our laboratory is directed toward this goal. Members of the LDLR superfamily also contain endocytic signals in their cytoplasmic domains. The presence of putative endocytic motifs in ST7's cytoplasmic tail suggests that, like other members of the superfamily, ST7 functions in endocytosis. In addition to putative internalization signals, we found that ST7's cytoplasmic domain contains several putative signal transduction motifs, as well as sites of potential phosphorylation (Figure 3 and Table 2). Their presence suggests that ST7 also plays a role in signal transduction. Recent studies show that several other LDLR family proteins function in signal transduction (*34*−*44*). The fact that ST7 localizes to the plasma membrane (Figure 4) is consistent with our hypothesis that ST7 functions as a plasma membrane receptor.

Figures 5 and 6 support the hypothesis that the cytoplasmic domain of ST7, like that of other members of the LDLR superfamily, functions in signal transduction. We recognize that in these experiments the proteins were overexpressed; therefore, the interactions observed do not imply that same interactions necessarily occur under normal expression conditions. However, RACK1 and SARA have been shown to be involved in signal transduction pathways. RACK1 was first identified as a shuttling protein for activated PKC (*23*, *24*). Because ST7's cytoplasmic tail contains six potential PKC phosphorylation sites (Table 2), it may be that RACK1 shuttles activated PKC to ST7 to phosphorylate it. RACK1 consists of seven WD domains that fold to form a β propeller structure (*45*). Such a structure may allow RACK1 to bind to several proteins simultaneously, thereby enabling it to function as a scaffold protein. Consistent with this, RACK1 has been shown to interact with a wide variety of proteins, in addition to PKC. These include the nonreceptor tyrosine kinases Src and Fyn (*25*, *46*−*48*), the cAMP-specific phosphodiesterase PDE4D5 (*49*), the Ras GTPase activating protein $p120^{GAP}$ (*50*), the angiotensin receptor associated protein AGTRAP (*51*), and the signal transducer and activator of transcription 1 protein (*52*). RACK1 also associates with the cytoplasmic domains of cell surface receptors such as β1 integrins (*53*), the insulin-like growth factor I receptor (*54*, *55*), the protein tyrosine phosphatase PTPμ (*56*), and the NR2B subunit of the *N*-methyl D-aspartate receptor (*48*). Because RACK1 interacts with a plethora of cellular proteins, it is believed to play a key role in regulating a variety of cellular signaling pathways (*25*).

The FYVE domain-containing protein SARA (also known as MADH-interacting protein) was first identified by Tsukazaki et al. (*27*). They found that SARA serves as a scaffold protein to link unphosphorylated SMAD2/3 to active TGFβ receptor heterodimers. By localizing SMAD2/3 to the membrane, SARA facilitates phosphorylation of these SMADs by the type I receptor's kinase domain (*27*). Phosphorylated SMAD2/3 dissociate from SARA and associate with SMAD4 to translocate to the nucleus and regulate gene expression. It was also determined that SARA localizes to early endosomes, suggesting that endocytosis plays a role in this SARA-mediated signal transduction pathway (*57*−*59*). Most recently, Hu et al. (*28*) reported that SARA plays a role in Rab5-mediated endocytosis. These data support the hypothesis that SARA plays a role in the endocytotic and/or signaling activity of ST7.

Although little is known about MIBP, it also appears to be involved in signal transduction. Li et al. (*26*) first identified MIBP using a yeast two-hybrid assay to screen for proteins that bind to the cytoplasmic tails of β1-integrins. They found that myocytes express a high level of MIBP prior to differentiation and a low level of MIBP after differentiation and that overexpression of MIBP in myocytes inhibits cell fusion and differentiation (*26*). Therefore, MIBP likely plays an important role in signal transduction pathways regulating myocyte fusion and differentiation.

Our data showing that ST7's cytoplasmic domain binds to proteins related to signal transduction are consistent with the emerging role of LDLR superfamily proteins as signal transducers (reviewed in refs *8*, *9*, *60*, and *61*). For example, Trommsdorff et al. (*34*, *35*) and D'Arcangelo et al. (*62*) demonstrated that VLDLR and ApoER2 are coreceptors for the extracellular protein Reelin. Binding of Reelin to these receptors has two major consequences, the internalization of Reelin and the activation of a tyrosine kinase signaling cascade. This results in the phosphorylation of Dab1 protein bound to the cytoplasmic domains of these receptors. Alterations in this pathway cause dysfunction in brain development (*35*). Additionally, several groups demonstrated that LRP5 and LRP6 participate in the Wnt signaling pathway (*37*−*40*, *63*). Both proteins serve as coreceptors for extracellular Wnt glycoproteins. Mao et al. (*40*) demonstrated that cytoplasmic domain of LRP5 binds to the scaffolding protein axin to promote β-catenin stabilization and Wnt responsive gene expression. Mice lacking LRP6 die at birth as a result of severe developmental defects, including malformation of the skeleton, limbs, eyes, and urogenital tract (*39*). Mutations in the human *LRP5* gene result in defects in bone density and eye development (*63*−*65*). Boucher et al.

(*42*) and Loukinova et al. (*43*) showed that LRP1 serves as a coreceptor for PDGF BB and that the adaptor protein Shc binds to a phosphotyrosine residue in LRP1's cytoplasmic domain upon PDGF BB stimulation. Finally, yeast two-hybrid studies demonstrated that the cytoplasmic tails of LRP1, LRP2, LDLR, VLDLR, and ApoER2 interact with proteins known to be involved in MAP kinase signal transduction, synaptic transmission regulation, cytoskeletal organization, cellular adhesion, and endocytosis, adding further support to the idea that members of the LDLR superfamily participate not only in endocytosis but also in signal transduction (*36*). The ST7-interacting proteins described in this paper can be classified into many of the same categories as those that interact with other LDLR superfamily members.

Our yeast two-hybrid studies also demonstrated that both SARA and MIBP bind to the juxtamembrane region of ST7's cytoplasmic domain (Figure 7 and Table 4). Because the bait construct containing ST7 residues 668−840 self-activated the yeast reporter genes, we cannot exclude the possibility that this region contains additional MIBP and SARA binding sites. Co-immunoprecipitation experiments to detect such binding sites in ST7 were unsuccessful because nonspecific bands obscured the area of interest. However, the presence of MIBP and SARA binding sites in the juxtamembrane region of ST7 supports our hypothesis that this region, which is highly conserved among the ST7 subfamily proteins, is important for ST7 function. Moreover, we determined that the first 10 amino acids of ST7's cytoplasmic domain might suffice for MIBP binding (Figure 8). On the basis of signal intensity, we conclude that the MIBP binds equally well to ST7 and $ST7_{tr1}$. Somewhat surprising was the fact that a small amount of $ST7_{tr2}$ associated with MIBP. Because the cytoplasmic tail of this truncated protein contains only one residue, we did not expect it to interact with MIBP. It is always possible that this band represents nonspecific antibody binding. However, because we failed to detect such nonspecific binding in other co-immunoprecipitation experiments using the V5 antibody, we interpret this band as a specific signal. The remaining lysine residue may play a critical role in the ST7-MIBP interaction, and by itself is able to interact with ST7, but does so much less efficiently. Another possible explanation is that residues of the transmembrane helix domain become exposed because of a conformational change when ST7 is active and participates in the ST7-MIBP interaction. The growth medium used in these studies may contain ligands that bind to ST7's extracellular domain to activate the receptor and induce such conformational changes. Studies of integrin cytoplasmic domains suggest that ligand binding does induce conformational changes that affect the position of residues within and near the membrane (*66*, *67*). Because the cells used in our co-immunoprecipitation experiments contain endogenous ST7 protein, it is possible that the latter protein was responsible for making it appear as if MIBP interacts with $ST7_{tr2}$. If dimerization of endogenous ST7 with $ST7_{tr2}$ were to occur, the observed interaction could have resulted from MIBP associating with the full-length cytoplasmic tail of endogenous ST7 instead of the truncated cytoplasmic tail. Therefore, immunoprecipitation of MIBP would cause both endogenous and truncated ST7 to be coprecipitated. This would seem to be the most likely explanation of our results with $ST7_{tr2}$. If dimerization explained that interaction, then it is possible that dimerization also explains the interaction between $ST7_{tr1}$ and MIBP. However, if it is responsible for both results, then we would have expected to see an equivalent amount of $ST7_{tr1}$ and $ST7_{tr2}$ pulled down by MIBP. This was not the case (Figure 8). Further studies are necessary to determine if ST7 dimerizes with itself.

Identification of the RACK1 binding site in ST7 proved to be more difficult using the yeast two-hybrid assay. Because RACK1 interacted with all of the ST7 bait proteins spanning residues 498−667, we were only able to determine that ST7 contains at least one RACK1 binding site in this region (Table 4 and Figure 7). A limitation of the yeast two-hybrid assay is that it is not quantitative. Therefore, it cannot be used to evaluate the strength of the interaction between RACK1 and the various ST7 bait proteins to more finely map RACK1's binding site on ST7. If there is only one binding site for RACK1 in this region, it must fall between residues 498−625 because these residues are common to all of the $ST7_{cyto}$ proteins that associate with RACK1. Moreover, the observation that RACK1 interacts with both $ST7_{cyto5}$ and $ST7_{cyto6}$, two bait proteins that do not include any common residues, suggests that each of these proteins contains part of the RACK1 binding site or that there is more than one RACK1 binding site in this region of ST7's cytoplasmic tail, and each of these bait proteins contain one or more complete sites. Moreover, because the yeast two-hybrid bait construct containing ST7 residues 668−840 ($ST7_{cyto3}$) was able to self-activate the yeast reporter genes, we cannot exclude the possibility that this region of ST7 contains additional RACK1 binding sites. Future co-immunoprecipitation experiments using ST7 proteins with various truncated cytoplasmic domains should clarify the manner in which ST7 interacts with RACK1.

ACKNOWLEDGMENT

We thank our colleagues Dr. Susanne Kleff for her valuable advice and her expert assistance with the yeast two-hybrid system and Dr. Kim Hien T. Dao for helpful discussions and assistance with immunoprecipitation experiments. The assistance of Emily Reamer with experiments and of Bethany Heinlen with the figures is deeply appreciated.

REFERENCES

1. McCormick, J. J., and Maher, V. M. (1994) Analysis of the multistep process of carcinogenesis using human fibroblasts, *Risk Anal. 14*, 257−263.
2. Qing, J., Wei, D., Maher, V. M., and McCormick, J. J. (1999) Cloning and characterization of a novel gene encoding a putative transmembrane protein with altered expression in some human transformed and tumor-derived cell lines, *Oncogene 18*, 335−342.
3. Ishii, H., Kim, D. H., Fujita, T., Endo, Y., Saeki, S., and Yamamoto, T. T. (1998) cDNA cloning of a new low-density lipoprotein receptor-related protein and mapping of its gene (LRP3) to chromosome bands 19q12−q13 2, *Genomics 51*, 132−135.
4. Krieger, M., and Herz, J. (1994) Structures and functions of multiligand lipoprotein receptors: macrophage scavenger receptors and LDL receptor-related protein (LRP), *Annu. Rev. Biochem. 63*, 601−637.
5. Hussain, M. M., Strickland, D. K., and Bakillah, A. (1999) The mammalian low-density lipoprotein receptor family, *Annu. Rev. Nutr. 19*, 141−172.

6. Strickland, D. K., Gonias, S. L., and Argraves, W. S. (2002) Diverse roles for the LDL receptor family, *Trends Endocrinol. Metab. 13*, 66−74.
7. Li, Y., Cam, J., and Bu, G. (2001) Low-density lipoprotein receptor family: endocytosis and signal transduction, *Mol. Neurobiol. 23*, 53−67.
8. Herz, J., and Bock, H. H. (2002) Lipoprotein receptors in the nervous system, *Annu. Rev. Biochem. 71*, 405−434.
9. van der Geer, P. (2002) Phosphorylation of LRP1: regulation of transport and signal transduction, *Trends Cardiovasc. Med. 12*, 160−165.
10. Sugiyama, T., Kumagai, H., Morikawa, Y., Wada, Y., Sugiyama, A., Yasuda, K., Yokoi, N., Tamura, S., Kojima, T., Nosaka, T., Senba, E., Kimura, S., Kadowaki, T., Kodama, T., and Kitamura, T. (2000) A novel low-density lipoprotein receptor-related protein mediating cellular uptake of apolipoprotein E-enriched β-VLDL in vitro, *Biochemistry 39*, 15817−15825.
11. Nielsen, H., Engelbrecht, J. S. B., Brunak, S., and von Heijne, G. (1997) Identification of prokaryotic and eukaryotic signal peptides and prediction of their cleavage sites, *Protein Eng. 10*, 1−6.
12. Claros, M. G., Brunak, S., and von Heijne, G. (1997) Prediction of N-terminal protein sorting signals, *Curr. Opin. Struct. Biol. 7*, 394−398.
13. Gattiker, A., Gasteiger, E., and Bairoch, A. (2002) ScanProsite: a reference implementation of a PROSITE scanning tool, *Appl. Bioinformatics 1*, 107−108.
14. Yamamoto, T., Davis, C. G., Brown, M. S., Schneider, W. J., Casey, M. L., Goldstein, J. L., and Russell, D. W. (1984) The human LDL receptor: a cysteine-rich protein with multiple Alu sequences in its mRNA, *Cell 39*, 27−38.
15. Bork, P., and Beckmann, G. (1993) The CUB domain. A widespread module in developmentally regulated proteins, *J. Mol. Biol. 231*, 539−545.
16. Christensen, E. I., and Birn, H. (2002) Megalin and cubilin: multifunctional endocytic receptors, *Nat. Rev. Mol. Cell Biol. 3*, 256−266.
17. Trowbridge, I. S., Collawn, J. F., and Hopkins, C. R. (1993) Signal-dependent membrane protein trafficking in the endocytic pathway, *Annu. Rev. Cell Biol. 9*, 129−161.
18. Kay, B. K., Williamson, M. P., and Sudol, M. (2000) The importance of being proline: the interaction of proline-rich motifs in signaling proteins with their cognate domains, *FASEB J. 14*, 231−241.
19. Blom, N., Gammeltoft, S., and Brunak, S. (1999) Sequence and structure-based prediction of eukaryotic protein phosphorylation sites, *J. Mol. Biol. 294*, 1351−1362.
20. Klingmuller, U., Bergelson, S., Hsiao, J. G., and Lodish, H. F. (1996) Multiple tyrosine residues in the cytosolic domain of the erythropoietin receptor promote activation of STAT5, *Proc. Natl. Acad. Sci. U.S.A. 93*, 8324−8328.
21. Sotgia, F., Lee, H., Bedford, M. T., Petrucci, T., Sudol, M., and Lisanti, M. P. (2001) Tyrosine phosphorylation of β-dystroglycan at its WW domain binding motif, PPxY, recruits SH2 domain containing proteins, *Biochemistry 40*, 14585−14592.
22. Macias, M. J., Wiesner, S., and Sudol, M. (2002) WW and SH3 domains, two different scaffolds to recognize proline-rich ligands, *FEBS Lett. 513*, 30−37.
23. Ron, D., Chen, C. H., Caldwell, J., Jamieson, L., Orr, E., and Mochly-Rosen, D. (1994) Cloning of an intracellular receptor for protein kinase C: a homologue of the β subunit of G proteins, *Proc. Natl. Acad. Sci. U.S.A. 91*, 839−843.
24. Ron, D., Jiang, Z., Yao, L., Vagts, A., Diamond, I., and Gordon, A. (1999) Coordinated movement of RACK1 with activated betaIIPKC, *J. Biol. Chem. 274*, 27039−27046.
25. Chang, B. Y., Chiang, M., and Cartwright, C. A. (2001) The interaction of Src and RACK1 is enhanced by activation of protein kinase C and tyrosine phosphorylation of RACK1, *J. Biol. Chem. 276*, 20346−20356.
26. Li, J., Mayne, R., and Wu, C. (1999) A novel muscle-specific β 1 integrin binding protein (MIBP) that modulates myogenic differentiation, *J. Cell Biol. 147*, 1391−1398.
27. Tsukazaki, T., Chiang, T. A., Davison, A. F., Attisano, L., and Wrana, J. L. (1998) SARA, a FYVE domain protein that recruits Smad2 to the TGFβ receptor, *Cell 95*, 779−791.
28. Hu, Y., Chuang, J. Z., Xu, K., McGraw, T. G., and Sung, C. H. (2002) SARA, a FYVE domain protein, affects Rab5-mediated endocytosis, *J. Cell Sci. 115*, 4755−4763.
29. Galliano, M. F., Huet, C., Frygelius, J., Polgren, A., Wewer, U. M., and Engvall, E. (2000) Binding of ADAM12, a marker of skeletal muscle regeneration, to the muscle-specific actin-binding protein, α-actinin-2, is required for myoblast fusion, *J. Biol. Chem. 275*, 13933−13939.
30. Salmikangas, P., Mykkanen, O. M., Gronholm, M., Heiska, L., Kere, J., and Carpen, O. (1999) Myotilin, a novel sarcomeric protein with two Ig-like domains, is encoded by a candidate gene for limb-girdle muscular dystrophy, *Hum. Mol. Genet. 8*, 1329−1336.
31. Hauser, M. A., Horrigan, S. K., Salmikangas, P., Torian, U. M., Viles, K. D., Dancel, R., Tim, R. W., Taivainen, A., Bartoloni, L., Gilchrist, J. M., Stajich, J. M., Gaskell, P. C., Gilbert, J. R., Vance, J. M., Pericak-Vance, M. A., Carpen, O., Westbrook, C. A., and Speer, M. C. (2000) Myotilin is mutated in limb girdle muscular dystrophy 1A, *Hum. Mol. Genet. 9*, 2141−2147.
32. Hauser, M. A., Conde, C. B., Kowaljow, V., Zeppa, G., Taratuto, A. L., Torian, U. M., Vance, J., Pericak-Vance, M. A., Speer, M. C., and Rosa, A. L. (2002) Myotilin Mutation Found in Second Pedigree with LGMD1A, *Am. J. Hum. Genet. 71*, 1428−1432.
33. Ilardi, J. M., Mochida, S., and Sheng, Z. H. (1999) Snapin: a SNARE-associated protein implicated in synaptic transmission, *Nat. Neurosci. 2*, 119−124.
34. Trommsdorff, M., Borg, J. P., Margolis, B., and Herz, J. (1998) Interaction of cytosolic adaptor proteins with neuronal apolipoprotein E receptors and the amyloid precursor protein, *J. Biol. Chem. 273*, 33556−33560.
35. Trommsdorff, M., Gotthardt, M., Hiesberger, T., Shelton, J., Stockinger, W., Nimpf, J., Hammer, R. E., Richardson, J. A., and Herz, J. (1999) Reeler/Disabled-like disruption of neuronal migration in knockout mice lacking the VLDL receptor and ApoE receptor 2, *Cell 97*, 689−701.
36. Gotthardt, M., Trommsdorff, M., Nevitt, M. F., Shelton, J., Richardson, J. A., Stockinger, W., Nimpf, J., and Herz, J. (2000) Interactions of the low density lipoprotein receptor gene family with cytosolic adaptor and scaffold proteins suggest diverse biological functions in cellular communication and signal transduction, *J. Biol. Chem. 275*, 25616−25624.
37. Wehrli, M., Dougan, S. T., Caldwell, K., O'Keefe, L., Schwartz, S., Vaizel-Ohayon, D., Schejter, E., Tomlinson, A., and DiNardo, S. (2000) Arrow encodes an LDL-receptor-related protein essential for Wingless signaling, *Nature 407*, 527−530.
38. Tamai, K., Semenov, M., Kato, Y., Spokony, R., Liu, C., Katsuyama, Y., Hess, F., Saint-Jeannet, J. P., and He, X. (2000) LDL-receptor-related proteins in Wnt signal transduction, *Nature 407*, 530−535.
39. Pinson, K. I., Brennan, J., Monkley, S., Avery, B. J., and Skarnes, W. C. (2000) An LDL-receptor-related protein mediates Wnt signaling in mice, *Nature 407*, 535−538.
40. Mao, J., Wang, J., Liu, B., Pan, W., Farr, G. H., III, Flynn, C., Yuan, H., Takada, S., Kimelman, D., Li, L., and Wu, D. (2001) Low-density lipoprotein receptor-related protein-5 binds to Axin and regulates the canonical Wnt signaling pathway, *Mol. Cell 7*, 801−809.
41. Barnes, H., Larsen, B., Tyers, M., and van Der Geer, P. (2001) Tyrosine-phosphorylated low-density lipoprotein receptor-related protein 1 (Lrp1) associates with the adaptor protein SHC in SRC-transformed cells, *J. Biol. Chem. 276*, 19119−19125.
42. Boucher, P., Liu, P., Gotthardt, M., Hiesberger, T., Anderson, R. G., and Herz, J. (2002) Platelet-derived growth factor mediates tyrosine phosphorylation of the cytoplasmic domain of the low-density lipoprotein receptor-related protein in caveolae, *J. Biol. Chem. 277*, 15507−15513.
43. Loukinova, E., Ranganathan, S., Kuznetsov, S., Gorlatova, N., Migliorini, M. M., Loukinov, D., Ulery, P. G., Mikhailenko, I., Lawrence, D. A., and Strickland, D. K. (2002) Platelet-derived growth factor (PDGF)-induced tyrosine phosphorylation of the low-density lipoprotein receptor-related protein (LRP). Evidence for integrated coreceptor function betwenn LRP and the PDGF, *J. Biol. Chem. 277*, 15499−15506.
44. Lutz, C., Nimpf, J., Jenny, M., Boecklinger, K., Enzinger, C., Utermann, G., Baier-Bitterlich, G., and Baier, G. (2002) Evidence of Functional Modulation of the MEKK/JNK/cJun Signaling Cascade by the Low-Density Lipoprotein Receptor-Related Protein (LRP), *J. Biol. Chem. 277*, 43143−43151.
45. Wall, M. A., Coleman, D. E., Lee, E., Iniguez-Lluhi, J. A., Posner, B. A., Gilman, A. G., and Sprang, S. R. (1995) The structure of the G protein heterotrimer Gi α 1 β 1 γ 2, *Cell 83*, 1047−1058.
46. Chang, B. Y., Conroy, K. B., Machleder, E. M., and Cartwright, C. A. (1998) RACK1, a receptor for activated C kinase and a homologue of the β subunit of G proteins, inhibits activity of src

tyrosine kinases and growth of NIH 3T3 cells, *Mol. Cell Biol. 18*, 3245−3256.
47. Chang, B. Y., Harte, R. A., and Cartwright, C. A. (2002) RACK1: a novel substrate for the Src protein-tyrosine kinase, *Oncogene 21*, 7619−7629.
48. Yaka, R., Thornton, C., Vagts, A. J., Phamluong, K., Bonci, A., and Ron, D. (2002) NMDA receptor function is regulated by the inhibitory scaffolding protein, RACK1, *Proc. Natl. Acad. Sci. U.S.A. 99*, 5710−5715.
49. Yarwood, S. J., Steele, M. R., Scotland, G., Houslay, M. D., and Bolger, G. B. (1999) The RACK1 signaling scaffold protein selectively interacts with the cAMP-specific phosphodiesterase PDE4D5 isoform, *J. Biol. Chem. 274*, 14909−14917.
50. Koehler, J. A., and Moran, M. F. (2001) RACK1, a protein kinase C scaffolding protein, interacts with the PH domain of p120GAP, *Biochem. Biophys. Res. Commun. 283*, 888−895.
51. Wang, W., Huang, Y., Zhou, Z., Tang, R., Zhao, W., Zeng, L., Xu, M., Cheng, C., Gu, S., Ying, K., Xie, Y., and Mao, Y. (2002) Identification and characterization of AGTRAP, a human homologue of murine Angiotensin II Receptor-Associated Protein (Agtrap), *Int. J. Biochem. Cell Biol. 34*, 93−102.
52. Usacheva, A., Smith, R., Minshall, R., Baida, G., Seng, S., Croze, E., and Colamonici, O. (2001) The WD motif-containing protein receptor for activated protein kinase C (RACK1) is required for recruitment and activation of signal transducer and activator of transcription 1 through the type I interferon receptor, *J. Biol. Chem. 276*, 22948−22953.
53. Liliental, J., and Chang, D. D. (1998) Rack1, a receptor for activated protein kinase C, interacts with integrin β subunit, *J. Biol. Chem. 273*, 2379−2383.
54. Hermanto, U., Zong, C. S., Li, W., and Wang, L. H. (2002) RACK1, an insulin-like growth factor I (IGF-I) receptor-interacting protein, modulates IGF-I-dependent integrin signaling and promotes cell spreading and contact with extracellular matrix, *Mol. Cell Biol. 22*, 2345−2365.
55. Kiely, P. A., Sant, A., and O'Connor, R. (2002) RACK1 is an insulin-like growth factor 1 (IGF-1) receptor-interacting protein that can regulate IGF-1-mediated Akt activation and protection from cell death, *J. Biol. Chem. 277*, 22581−22589.
56. Mourton, T., Hellberg, C. B., Burden-Gulley, S. M., Hinman, J., Rhee, A., and Brady-Kalnay, S. M. (2001) The PTPmu protein-tyrosine phosphatase binds and recruits the scaffolding protein RACK1 to cell−cell contacts, *J. Biol. Chem. 276*, 14896−14901.
57. Itoh, F., Divecha, N., Brocks, L., Oomen, L., Janssen, H., Calafat, J., Itoh, S., and Dijke Pt, P. (2002) The FYVE domain in Smad anchor for receptor activation (SARA) is sufficient for localization of SARA in early endosomes and regulates TGF-β/Smad signaling, *Genes Cells 7*, 321−331.
58. Penheiter, S. G., Mitchell, H., Garamszegi, N., Edens, M., Dore, J. J., Jr., and Leof, E. B. (2002) Internalization-dependent and -independent requirements for transforming growth factor β receptor signaling via the Smad pathway, *Mol. Cell Biol. 22*, 4750−4759.
59. Hayes, S., Chawla, A., and Corvera, S. (2002) TGFβ receptor internalization into EEA1-enriched early endosomes: role in signaling to Smad2, *J. Cell Biol. 158*, 1239−1249.
60. Strickland, D. K., Kounnas, M. Z., and Argraves, W. S. (1995) LDL receptor-related protein: a multiligand receptor for lipoprotein and proteinase catabolism, *FASEB J. 9*, 890−898.
61. Herz, J., and Strickland, D. K. (2001) LRP: a multifunctional scavenger and signaling receptor, *J. Clin. Invest. 108*, 779−784.
62. D'Arcangelo, G., Homayouni, R., Keshvara, L., Rice, D. S., Sheldon, M., and Curran, T. (1999) Reelin is a ligand for lipoprotein receptors, *Neuron. 24*, 471−479.
63. Gong, Y., Slee, R. B., Fukai, N., Rawadi, G., Roman-Roman, S., Reginato, A. M., Wang, H., Cundy, T., Glorieux, F. H., Lev, D., Zacharin, M., Oexle, K., Marcelino, J., Suwairi, W., Heeger, S., Sabatakos, G., Apte, S., Adkins, W. N., Allgrove, J., Arslan-Kirchner, M., Batch, J. A., Beighton, P., Black, G. C., Boles, R. G., Boon, L. M., Borrone, C., Brunner, H. G., Carle, G. F., Dallapiccola, B., De Paepe, A., Floege, B., Halfhide, M. L., Hall, B., Hennekam, R. C., Hirose, T., Jans, A., Juppner, H., Kim, C. A., Keppler-Noreuil, K., Kohlschuetter, A., LaCombe, D., Lambert, M., Lemyre, E., Letteboer, T., Peltonen, L., Ramesar, R. S., Romanengo, M., Somer, H., Steichen-Gersdorf, E., Steinmann, B., Sullivan, B., Superti-Furga, A., Swoboda, W., van den Boogaard, M. J., Van Hul, W., Vikkula, M., Votruba, M., Zabel, B., Garcia, T., Baron, R., Olsen, B. R., and Warman, M. L. (2001) LDL receptor-related protein 5 (LRP5) affects bone accrual and eye development, *Cell 107*, 513−523.
64. Little, R. D., Carulli, J. P., Del Mastro, R. G., Dupuis, J., Osborne, M., Folz, C., Manning, S. P., Swain, P. M., Zhao, S. C., Eustace, B., Lappe, M. M., Spitzer, L., Zweier, S., Braunschweiger, K., Benchekroun, Y., Hu, X., Adair, R., Chee, L., FitzGerald, M. G., Tulig, C., Caruso, A., Tzellas, N., Bawa, A., Franklin, B., McGuire, S., Nogues, X., Gong, G., Allen, K. M., Anisowicz, A., Morales, A. J., Lomedico, P. T., Recker, S. M., Van Eerdewegh, P., Recker, R. R., and Johnson, M. L. (2002) A mutation in the LDL receptor-related protein 5 gene results in the autosomal dominant high-bone-mass trait, *Am. J. Hum. Genet. 70*, 11−19.
65. Boyden, L. M., Mao, J., Belsky, J., Mitzner, L., Farhi, A., Mitnick, M. A., Wu, D., Insogna, K., and Lifton, R. P. (2002) High bone density due to a mutation in LDL-receptor-related protein 5, *N. Engl. J. Med. 346*, 1513−1521.
66. Armulik, A., Nilsson, I., von Heijne, G., and Johansson, S. (1999) Determination of the border between the transmembrane and cytoplasmic domains of human integrin subunits, *J. Biol. Chem. 274*, 37030−37034.
67. Lu, C., Takagi, J., and Springer, T. A. (2001) Association of the membrane proximal regions of the α and β subunit cytoplasmic domains constrains an integrin in the inactive state, *J. Biol. Chem. 276*, 14642−14648.

BI034081Y